

Optical amplifiers and lasers based on tapered fiber geometry for power and energy scaling with low signal distortion

Valery Filippov*^a, Yuri K. Chamorovskii^b, Konstantin M. Golant^b, Andrei Vorotynskii^a, Oleg G. Okhotnikov^a,

^aTampere University of Technology, 33101 Tampere, Finland; ^bKotel'nikov Institute of Radio Engineering and Electronics, Mokhovaya 11, bld.7, 125009 Moscow, Russian Federation

ABSTRACT

We report theoretical and experimental study of tapered double-clad fibers (T-DCF) and consider various amplifiers and lasers using this fiber as a gain medium.

Keywords: Fiber lasers and amplifiers, active fibers, tapered fibers

1. INTRODUCTION

Amplifiers and lasers employed tapered double-clad fiber (T-DCF) as a gain medium exhibit numerous unique advantages compared with regular active fibers. Primarily, T-DCF with large modal size and core diameter at taper end up to 200 μm could generate nearly ideal beam quality with low non-linear phase shift (B-integral) and is capable of high energy storage. The clad diameter of T-DCF up to 1.6 mm allows pumping by inexpensive powerful low brightness laser diode bars. The axial variation of taper diameter is accompanied by several attractive mechanisms which assist signal propagation. The variation of transverse size of the fiber taper results in a higher pump absorption due to improved clad mode mixing in T-DCF. Tapering of gain fiber also causes an efficient ASE suppression for amplification of low duty cycle pulses. Axially non-uniform geometry of taper increases significantly the SBS threshold for nanosecond pulses amplification. We have found recently that the threshold of the modal instability of T-DCF amplifier increases significantly due to small difference between propagation constants of interfering modes.

We have experimentally demonstrated several amplifiers and lasers using ytterbium T-DCF gain fiber in the present paper. High power CW one-stage amplifier with 46 dB gain and nanosecond actively Q-switched laser produced 1.6 mJ pulse energy are presented as example of T-DCF applications. The picosecond all-fiber tapered MOPA system with record 0.3 mJ out-of-fiber pulse energy is described in details.

2. PROPERTIES AND ADVANTAGES OF T-DCF

The main advantages of T-DCF fibers compared with common LMA fibers are:

- Large mode size;
- Higher absorption per unit length;
- Intrinsic built-in mechanism for ASE suppression;
- Steady mode instability;
- High factor of brightness increase.

*valery.filippov@tut.fi, phone +358 40 198 1055

2.1. Mode size in T-DCF

One of the main advantages of T-DCF is unprecedentedly large mode size combined with single mode propagation regime in a taper section of increased diameter. There are few types of optical fibers that allow large mode size to be achieved. Among them fibers with low numerical apertures below 0.05 are widely used. The 40-50 μm limits for fiber diameter are determined by the current technology which dictates the smallest achievable index step. Another approach for fabrication large modal sizes is based on the so-called 3C fibers where higher-order modes outcoupling from the multimode core is made through coupling with additional waveguides located in a cladding and providing modal selection for fundamental mode. Highest mode diameters of the core achievable in these fibers are 50-60 μm . In microstructure fibers, e.g. rod-type fibers, core diameter can be increased up to 130 μm . However, these fibers are extremely sensitive to bending; consequently, they need to be positioned in a straight line during application procedure.

Active tapered fibers with double cladding (T-DCF) allow for substantial increase of mode diameter, i.e. it still can be considered as an ordinary fiber which can be coiled in a usual way. Recently, we have demonstrated the single mode propagation in a tapered fiber with core diameter of 120 μm ^{1,2}. We have developed an active tapered fiber with core diameter in a large size section of 200 μm and aperture of 0.11. Fig. 1 shows parameters of active taper: photograph of cross-section, longitudinal variation of fiber diameter and results of M^2 measurements. Experimental results confirm that tapered fiber with core diameter of 200 μm ($V=70$, total number of propagating modes ~ 2000) supports single mode with $M^2=1.4$. The method using S^2 technique, also confirm the single mode propagation

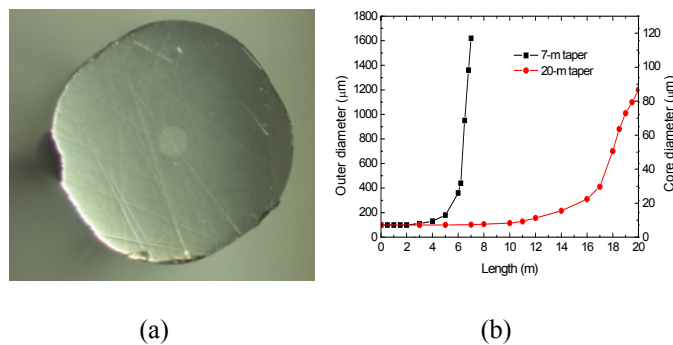


Fig.1. (a) Picture of T-DCF end face 190/1460 μm and (b) longitudinal profile distribution.

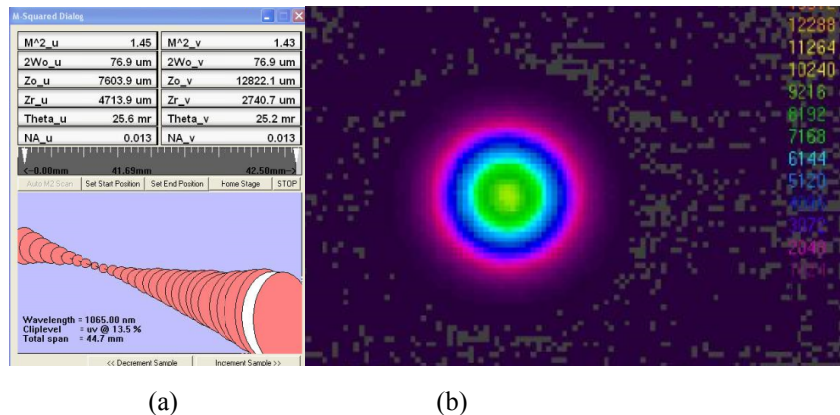


Fig.2. Results on M^2 measurements (a) and transverse beam distribution (b).

Essential feature responsible for the single mode operation of the taper is a transverse distribution of the core index. We have recently shown in Ref.², that for large core diameters, the transverse beam profile has distribution similar to the distribution of the core index. The circularly deep in a core index profile, therefore, results in a ring-like intensity

distribution². Gaussian beam profile requires preform with step-index or gradient index free from parasitic index variations since preform index profile follows the index distribution. Beam quality in a tapered fiber depends largely on core index profile of the preform, i.e. profile distribution without significant index modulation.

2.2. High absorption per unit length

It is well known that in powerful fiber lasers (amplifiers) short fibers with a high concentration of rare earth dopants are typically used to reduce the nonlinear effects. Increasing of the dopant concentration has certain limits, since it could lead to photodarkening of active fibers due to clasterization. T-DCF active double-clad fibers exhibit significantly larger absorption per unit length compared to a regular cylindrical fiber made from the same preform and provides the same brightness of the output radiation.

T-DCF always has higher absorption per unit length (in the wide taper end), as the "center of gravity" of the distribution of the dopants in the fiber is shifted towards the wide end. As we have shown experimentally earlier², there is no difference in terms of beam quality and brightness between emission from wide and narrow side of the T-DCF. The brightness of the output radiation generated or amplified by tapered fiber is equivalent to the regular (cylindrical) fiber and has parameters similar to that of narrow section of T-DCF.

Absorption in the T-DCF is determined mainly by the amount of dopants in the core and the core/cladding aspect ratio. Fig. 3 shows the ratio of the lengths of conventional fiber and T-DCF with a linear profile with the same number of dopants in the core and the same brightness (the same narrow part) as a function of the tapering ratio.

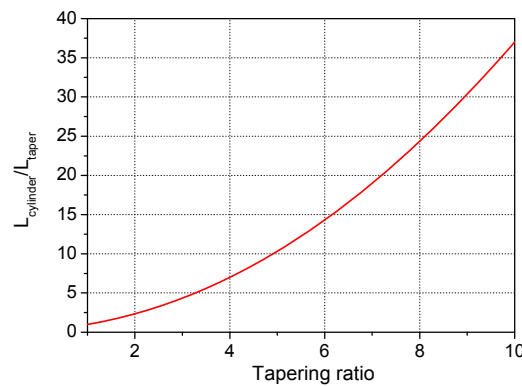


Fig.3. The ratio of lengths of volume-equivalent cylindrical and tapered fibers versus tapering ratio.

As can be seen from Fig.3, the tapering ratio of 5 enables an order of magnitude shorter T-DCF compared with a regular cylindrical fiber. Earlier⁴ we have made a comparative numerical analysis of the propagation, pump absorption and light generation of radiation in the laser containing tapered and equivalent cylindrical fiber. The results are shown in Fig. 4.

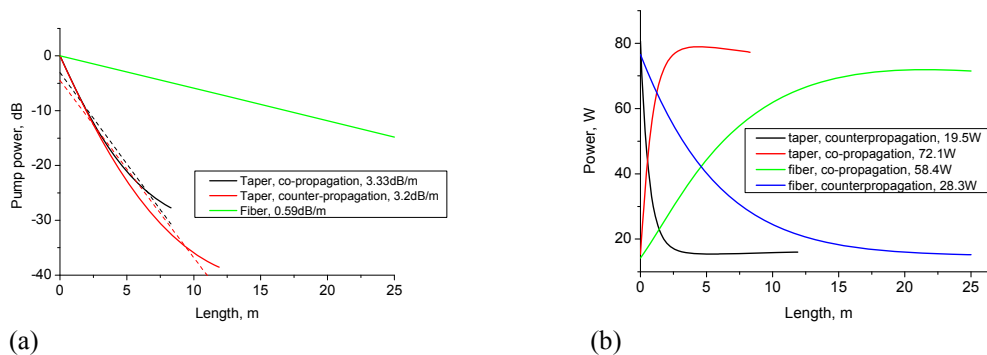


Fig. 4. Longitudinal distribution of pump (a) and signal (b) power. Pump power is 100 W at 920 nm.

2.3. Intrinsic built-in mechanism of ASE suppression

The degradation of the pulse train contrast during amplification of low duty cycle pulses represents a significant problem. The decay of pulse train quality occurs due to accumulation of ASE between the pulses as a result of high gain and low repetition rate. The ASE storage leads to a high level of CW background radiation, which degrades the contrast of the output pulse sequence. This feature represents the main mechanism preventing generation of short pulses with low duty cycle, e.g. for repetition frequency below several hundred kilohertz.

Amplifying taper allows significantly reduce the negative impact of ASE as compared with uniform fiber amplifier. Indeed, as it has been shown previously⁴, ASE accumulation occurs during the interval between the pulses and it propagates only in direction from the narrow toward wide end of the tapered amplifier. ASE radiation propagating in the opposite direction (from the wide to narrow end), undergoes loss⁴:

$$L_l = 20 \cdot \log(d_1/d_2)[dB], \quad (1)$$

where l is distance to the narrow end of T-DCF, d_1 and d_2 are core diameters at the arbitrary location and at the narrow end of the taper.

ASE emitted only within the aperture of $NA_t = NA \cdot d_2/d_1$ could reach the narrow end of T-DCF which reduces significantly the overall level of ASE radiation. Thus, as it follows from (1), tapering the fiber by factor of 10, leads to the suppression of the ASE propagated in the opposite direction by 20dB. As it will be shown below, the mechanism of ASE suppression allows to reduce significantly the repetition rate (up to CW radiation) of amplified/generated pulses.

2.4. Suppression of intermodal interference and SBS

Usually, double-clad fibers are multimode fibers both in the core and in the cladding. Consequently, intermodal interference causes a modal instability and modal noise in lasers and amplifiers based on double-clad fiber. Earlier, we have shown³, that this effect could be very significant, particularly, active fiber length modulation with amplitude of 10 μm leads to intensity modulation with depth of 0.6%. Amplitudes of n -th harmonics of the intensity due to the intermodal interference signals are proportional to the propagation constants difference of the interfering modes³:

$$I_{2n\Omega} \sim \cos(\beta_i - \beta_j)L \cdot J_{2n}((\beta_i - \beta_j) \cdot \Delta L) \sim J_{2n}((\beta_i - \beta_j) \cdot \Delta L) \quad (2)$$

$$I_{(2n-1)\Omega} \sim \sin(\beta_i - \beta_j)L \cdot J_{2n-1}((\beta_i - \beta_j) \cdot \Delta L) \sim (\beta_i - \beta_j)L \cdot J_{2n-1}((\beta_i - \beta_j) \cdot \Delta L) \quad (3)$$

, where β_i propagation constant of mode with index i , L – total fiber length, ΔL – amplitude of fiber's length modulation with frequency Ω and J_n is Bessel function.

Accordingly, to minimize the difference of propagation constants, we should minimize the impact of intermodal interference. With this approach, we can minimize the impact of intermodal interference by using of a tapered fiber. Indeed, the tapered fiber could be represented as a continuous transition between the waveguide, where several modes can propagate with propagation constants $\beta_1 \beta_2 \dots \beta_n$, and free space, where only a plane wave could propagate with the propagation constant $k_0 = 2\pi n/\lambda$:

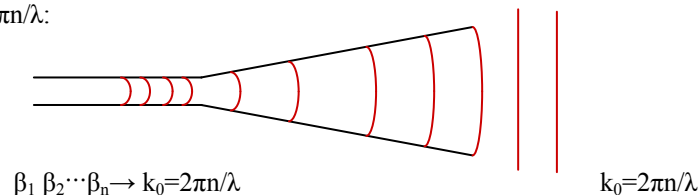


Fig.5. Mode propagation in the tapered fiber

Accordingly, the propagation through a tapered fiber changes the propagation constants of the modes so that the difference between them approaches zero, as it has been shown in Fig.6.

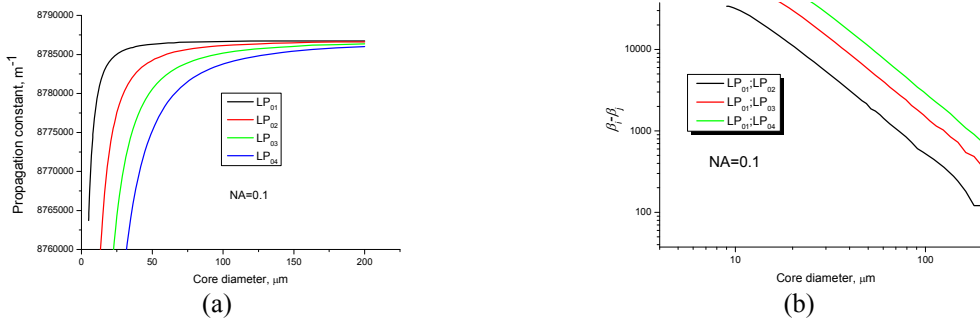


Fig.6. Propagation constant (a) and difference between propagation constants (b) as a function of core diameter.

As it follows from the results of calculations (Fig.6), the difference in between the propagation constants of LP01 and LP02 modes is decreased by more than 2 orders of magnitude with an increasing of core diameter from 10 to 200 μm. We have confirmed experimentally these calculations by demonstration of 500 W fiber laser with T-DCF3 free from any mode instability.

2.5. High brightness magnification factor

Fiber lasers (amplifiers) with a double-clad fiber (DCF) are efficient devices for improving the pump light brightness. For DCF with core and clad areas of A_{core} and A_{clad} , respectively, the achievable brightness magnification factor by a laser(amplifier) can be given by:

$$K_{DCF} = S \cdot \frac{A_{clad}}{A_{core}} \cdot \left(\frac{NA_{clad}}{NA_{core}} \right)^2 = S \cdot \left(\frac{D_{clad} \cdot NA_{clad}}{D_{core} \cdot NA_{core}} \right)^2 \quad (3)$$

,where S slope efficiency of a laser (amplifier), NA_{clad} и NA_{core} are numerical apertures of cladding and core, respectively, D_{clad} and D_{core} are diameters of cladding and core.

For a standard DCF fiber (e.g. Liekki Yb1200) with a 20 μm core diameter, 400 μm cladding, and NA of core and clad of 0.06 and 0.46, respectively, the K_{DCF} factor is about 3000.

As it was noted above, the brightness of the output radiation of T-DCF launched via its wide end is determined by core parameters at the narrow end. Accordingly, the brightness magnification factor of T-DCF is determined by⁴:

$$K_{T-DCF} = S \cdot \frac{A_{clad_input}}{A_{core_output}} \cdot \left(\frac{NA_{launch}}{NA_{core}} \right)^2 = S \cdot \left(\frac{T \cdot D_{clad_output} \cdot NA_{launch}}{D_{core_output} \cdot NA_{core}} \right)^2 = T^2 \cdot F^2 \cdot K_{DCF} \quad (4)$$

,where T – tapering ratio and, F is NA fill factor.

As it follows from (4), the brightness magnification factor for T-DCF is higher than for regular DCF fiber, when $T > 1/F$, that is usual situation.

3. T-DCF-BASED LASERS AND AMPLIFIERS

Next some schemes of lasers and amplifiers using active tapered fibers are considered.

3.1. CW high power and high gain amplifier with T-DCF

We have investigated the CW T-DCF amplifier in two regimes: for a narrowband and broadband signal amplification⁵. The experimental set up of CW single-stage amplifier with T-DCF active fiber is shown in Fig. 7. The narrow-band seed source is CW fiber laser⁵. The dependence of the output power of the amplifier versus pumping power is shown in Fig. 8 (black squares). Fig. 8 also shows the backscattered radiation from the launched pump power (open circles). The experimental results show that the level of backscattered radiation is below the level of the amplified signal by more than 50 dB.

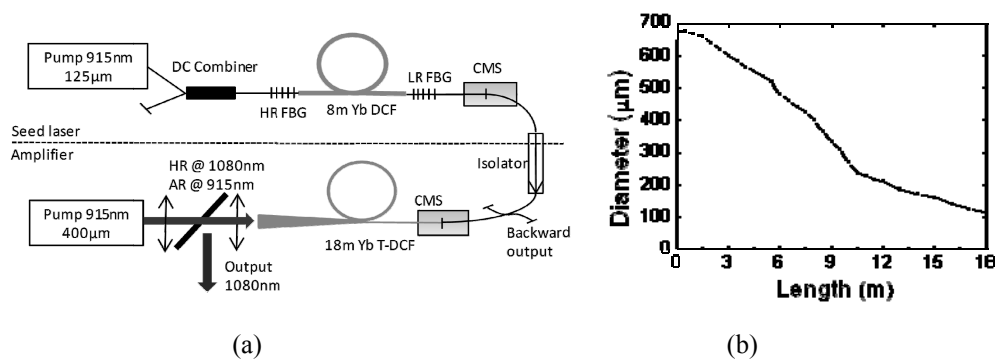


Fig.7. (a) The experimental set up of T-DCF fiber amplifier and (b) outer diameter of the T-DCF versus length.

The dependence of the output power versus the launched pump power is linear, without any signs of saturation. The image of output beam for core diameter 43 μm and $M^2=1.06$ is shown in the in Fig.8, as an inset.

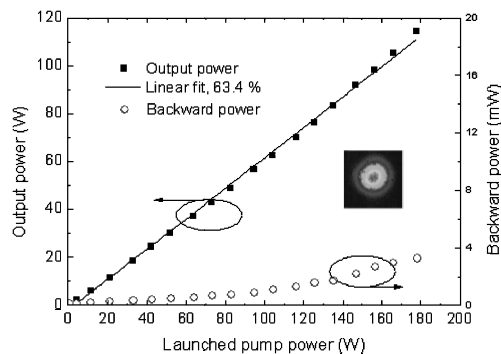


Fig.8. The output power and backward power versus launched pump power for $P_{\text{seed}}=0.49$ W. The inset shows the output beam image.

The gain dependence on the seed output power is shown in Figure 9. The maximum gain is about 25 dB for the output power of 110 W.

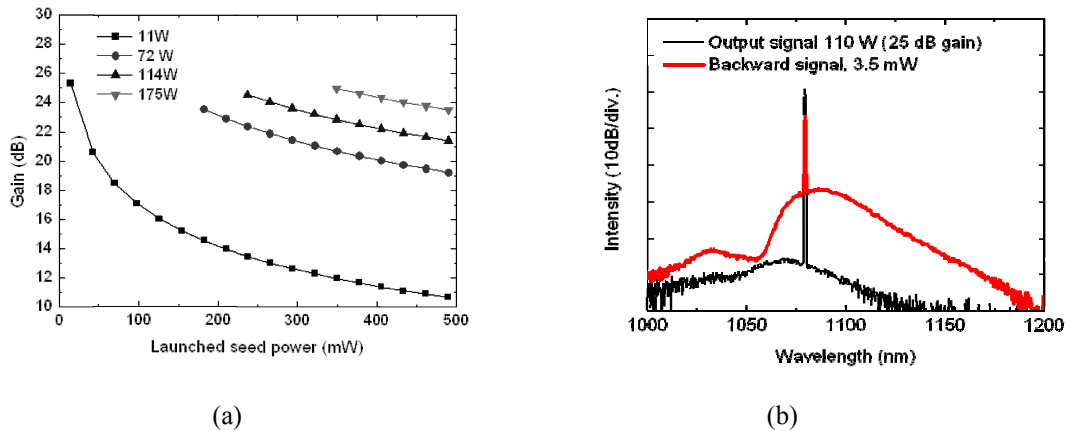


Fig. 9. Gain as function of seed signal power (a) and optical spectra of the forward (black) and backward (red) signals with the narrowband seed signal at maximum output power and gain.

The magnitude of the gain is limited by the setup of parasitic pulsing. Initially, backscattered radiation is determined preferably by the Rayleigh scattering. However, with further increasing of the output power, the threshold of SBS is reached and pulsing occurs representing the limiting factor of the output power. It should be noted that the threshold for SBS and corresponding pulsing is substantially higher (~25 dB) compared with conventional amplifiers, where it is usually of 20 dB.

High gain is defined by the T-DCF intrinsic properties. Primarily, the SBS threshold is increased due to the existing core modulation⁶, and secondly, the backscattered radiation suffers additional losses due to vignetting effect.

In a separate experiment, we have investigated the influence of the seed source bandwidth on the operation of the amplifier. The broadband seed source has been build up with a 15 nm FWHM bandwidth and 100 mW output power. Fig.10 shows the dependence of the output power (a) and the gain (b) of the amplifier versus seed power for two values of the pump power (11 and 32W).

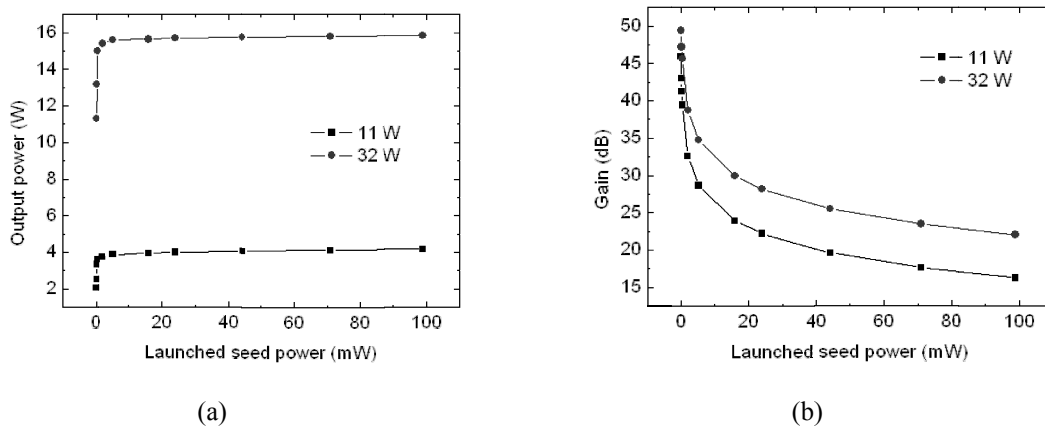


Fig. 10. (a) The dependance of output power as function of power of broadband input signal and (b) gain as a function of launched seed power for two values of pump power.

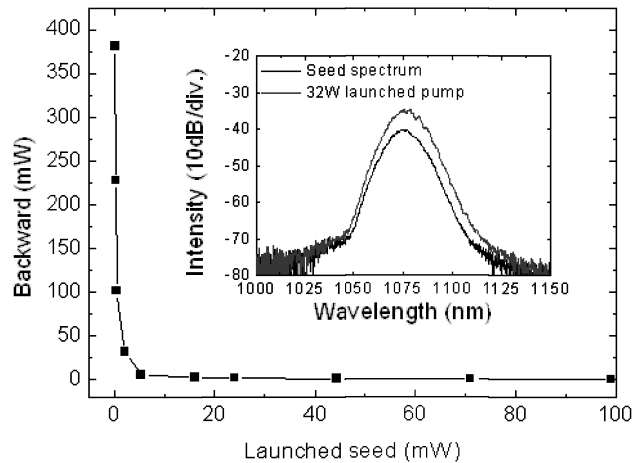


Fig. 11. Backward power versus launched seed power for broadband input signal at 32 W of pump power, and the output spectrum at the input and output of the amplifier (inset).

Fig.11 shows the power of backscattered emission versus the power of seed source (32 W pump power). Results shown in Fig. 10 and 11 indicate that the reduction of the seed power below 0.5 mW leads to a sharp increase of the backscattered radiation. This is due to the fact that low input power is not sufficient for the amplifier saturation. However, for 0.5 mW of input seed power and by pumping the amplifier with 32 W, 15 W of measured output corresponds to the 46 dB gain.

3.2. Actively Q-switched tapered fiber laser

The experimental setup of the Q-switched tapered fiber laser used in the experiments is shown in Fig.12⁷.

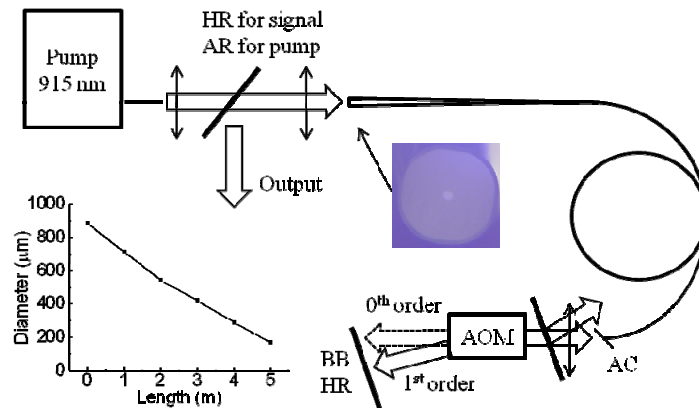


Fig.12. Experimental set up of the Q-switched tapered fiber laser setup. Micrograph of the wide fiber end, and the longitudinal profile of the T-DCF are shown in the Figure.

The T-DCF was end-pumped by a fiber-coupled laser diode bar at 915 nm through the wide fiber end. The laser cavity was formed by Fresnel reflection from the wide fiber end and by a broadband (BB) high-reflective (HR) mirror. Active Q-switching was achieved by an acousto-optic modulator (AOM) placed between the narrow end of T-DCF and the HR mirror, which reflected the 1st diffraction order back to the cavity. A 1- μ m edge filter was placed between the fiber and the AOM to filter out unabsorbed pump, which reduces the thermal load on the modulator.

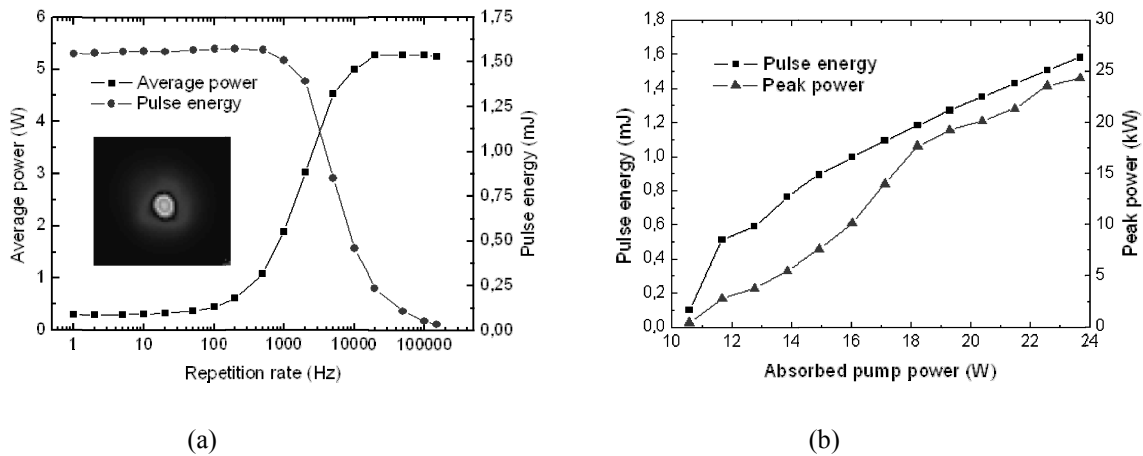


Fig. 13. Pulse energy and average power (including ASE) versus repetition rate at a constant pump power (a) and . The output beam profile with $M^2 = 2.7$ is shown as an inset.

Pulse energy of 1.58 mJ, corresponding to a peak power of 24.3 kW has been achieved. Above this value, irregular backward-propagating pulses and pulse breakdown were observed. Independently of pump power, single-shot operation was also achieved by manually triggering the AOM control pulse, without notable changes in pulse energy or pulse shape.

3.3. Ytterbium picosecond MOPA with T-DCF

The scheme of picosecond fiber MOPA is shown in Figure 14. As a seed source, we used a SESAM based mode locked fiber laser. The laser emits pulses with duration from 5 to 80 ps depending on the cavity details. The repetition rate was changed between 20 and 40 MHz at the wavelength of 1040 nm. The light from the seed was amplified by two core pumped amplifiers. To reduce a repetition rate, we used AOM-based pulse picker. The buster amplifier used 6-m long T-DCF with total absorption of 15 dB at 976 nm wavelength. T-DCF has a parabolic longitudinal shape, with the 100 μm core diameter at the wide side ($NA_{\text{core}}=0.11$). The output beam has a Gaussian shape with measured of $M^2=1.22$.

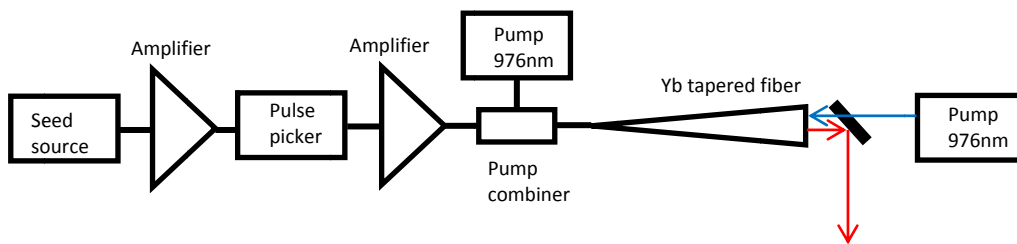


Fig.14. The experimental set up of picosecond MOPA

TDC-F was pumped from both narrow and wide side. In the experiment, we measured the energy of the output pulses with an Ophir PE9F detector as a function of the pump power launched into the wide end. A typical dependence of 60 ps output pulse energy on the launched pump power is shown in Fig.15.

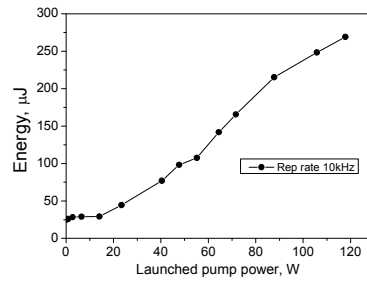


Fig. 15. Pulse energy for 60 ps duration and 10 kHz repetition rate versus launched pump power.

Typical spectra of seeded (red line) and the amplified (black) signals are shown in Fig. 16 (a). Fig.16b shows the autocorrelation of the amplified 20 ps pulse.

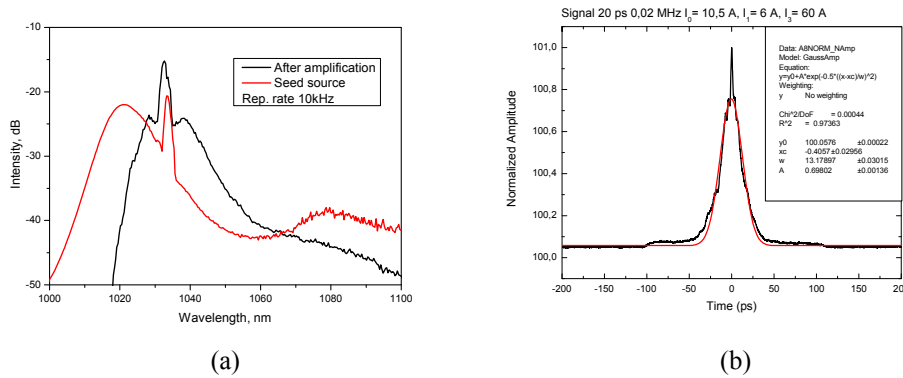


Fig.16. (a) Spectra of seed source (red line) and amplified at T-DCF emission; (b) temporal shape of amplified 20ps pulse.

The highest pulse energy obtained in the experiment was 280 μJ for 60 ps pulse duration at repetition rate of 10 kHz, which corresponds to 5 MW of peak power.

4. CONCLUSION

The presented paper overviews the basic properties of active T-DCF utilized as a medium for light amplification and generation. We have shown that T-DCF has a number of unique properties that allow to avoid non-linear effects during light amplification and generation. CW single stage amplifier using T-DCF demonstrates the record high gain of 46 dB in the saturated regime and output beam quality of $M^2=1.06$. T-DCFs allows to build a simple and powerful nanosecond pulsed laser. Finally, we have demonstrated all-fiber picosecond amplifier with 0.28 mJ of output pulse energy and 5 MW peak power.

REFERENCES

- [1] J. Kerttula, V. Filippov, V. Ustimchik, Y. Chamorovskiy, O. G. Okhotnikov, "Fundamental mode evolution in long, large-core ($>100 \mu\text{m}$) adiabatic tapers", Photonics West 2013-LASE: Lasers and Sources, 2-7 February 2013, San Francisco, CA, USA, pp. 860121-1-860121-8.

- [2] J. Kerttula, V. Filippov, V. Ustimchik, Y. Chamorovskiy, O. G. Okhotnikov, "*Mode evolution in long tapered fibers with high tapering ratio*", Optics Express, vol.20, issue 23, pp.25461-25470, (2012)
- [3] V. Filippov, V. Ustimchik, Yu. Chamorovskii, K. Golant, A. Vorotynskii and O. G. Okhotnikov "Impact of Axial Profile of the Gain Medium on the Mode Instability in Lasers: Regular Versus Tapered Fibers", CLEO/Europe-EQEC 2015, June 21-25.
- [4] J. Kerttula, V. Filippov, Y. Chamorovskii, V. Ustimchik, K. Golant, O. G. Okhotnikov, "Principles and Performance of Tapered Fiber Lasers: from Uniform to Flared Geometry", Applied Optics, vol.51, issue 29, pp.7025-7038, (2012).
- [5] J. Kerttula, V. Filippov, Y. Chamorovskii, V. Ustimchik, K. Golant, O. G. Okhotnikov, "Tapered fiber amplifier with high gain and output power", Laser Physics vol.22, No.11, pp.1734-1738 (2012)
- [6] K. Shiraki, M. Ohashi and M. Tateda, "Suppression of stimulated Brillouin scattering in a fiber by changing the core radius", Electronics Letters vol.31, No.8, pp.668-669 (1995).
- [7] J. Kerttula, V. Filippov, Yu. Chamorovskii, K. Golant, and O. G. Okhotnikov, "Actively Q-switched 1.6-mJ tapered double-clad ytterbium-doped fiber laser," Opt. Express 18, 18543-18549 (2010).